

## Effects of random fields in an antiferromagnetic Ising spin glass

Selma R. Vieira and Fernando D. Nobre

*Departamento de Física Teórica e Experimental, Universidade Federal do Rio Grande do Norte,  
Caixa Postal 1641, 59072-970 Natal, RN, Brazil*

Carlos S. O. Yokoi

*Instituto de Física, Universidade de São Paulo, Caixa Postal 66318, 05315-970 São Paulo, SP, Brazil*

(Received 26 July 1999; revised manuscript received 30 November 1999)

The effects of random fields on the two-sublattice infinite-ranged Ising spin-glass model are investigated. This model is expected to be appropriate as a mean-field description of antiferromagnetic spin glasses such as  $\text{Fe}_x\text{Mn}_{1-x}\text{TiO}_3$ . Within replica-symmetric calculations, we study the influence of Gaussian and bimodal random fields on the phase transitions and phase diagrams. It is shown that, in the presence of random fields, the first-order transitions are weakened and may become continuous. Also, the antiferromagnetic phases are always destroyed by sufficiently strong random fields. A qualitative comparison with existing experimental results and the limitations of the present calculations are discussed.

PACS number(s): 05.50.+q, 64.60.-i, 75.10.Nr, 75.50.Lk

### I. INTRODUCTION

Experimental works carried out in diluted antiferromagnets (e.g.,  $\text{Fe}_x\text{Mg}_{1-x}\text{Cl}_2$  [1–3]) and in mixed antiferromagnetic compounds (e.g.,  $\text{Fe}_x\text{Mn}_{1-x}\text{TiO}_3$  [4,5]) show evidences of spin-glass behavior for certain range of  $x$  values. Within such concentration ranges, these systems may be regarded as Ising short-ranged spin glasses: the competing short-range ferromagnetic and antiferromagnetic interactions are responsible for frustration, while the strong uniaxial anisotropy keeps the spins aligned along the axial direction. A two-sublattice version of the infinite-ranged Sherrington-Kirkpatrick (SK) spin-glass model [6] was proposed [7–10], as a mean-field theory to explain the antiferromagnetic and spin-glass orderings observed in these systems. The transition to the antiferromagnetic phase is characterized by the onset of the staggered magnetization [11], whereas the transition to the spin-glass phase is signaled by the instability of the replica-symmetric solution [12]. In the spin-glass phase the appropriate solution has a broken replica symmetry [13,14], describing a nonergodic situation, with a free-energy profile with many valleys separated by large barriers. Thus, experimentally the transition to the spin-glass phase is often identified with the occurrence of irreversibility and hysteresis. Experimental determination of the field-temperature phase diagram in  $\text{Fe}_x\text{Mn}_{1-x}\text{TiO}_3$  [15], as well as the de Almeida-Thouless instability line [12], are in qualitative agreement with mean-field results [10].

Random fields are generated in diluted antiferromagnets through the application of an external uniform magnetic field [16,17]. Indeed, both spin-glass [1] and random-field [18] behaviors have been reported in  $\text{Fe}_x\text{Mg}_{1-x}\text{Cl}_2$ . The mixed compound  $\text{Fe}_x\text{Mn}_{1-x}\text{TiO}_3$  is not diluted, but it has been argued that the imbalance between the magnetic moments of Fe and Mn will also generate an effective random field [15]. In contrast to these systems, the diluted antiferromagnet  $\text{Fe}_x\text{Zn}_{1-x}\text{F}_2$  presents almost no frustration and only the random-field behavior was observed at small dilutions [19]. However, according to recent theoretical investigations

[20,21], small frustration plays an important role at high dilutions, leading to the occurrence of spin-glass behavior, as reported by experimental studies [22,23].

Such considerations motivated us to study the effects of random fields on the two sublattice SK model [7–10]. In particular, we will be interested in the effects of the random fields on the phase transitions and phase diagrams of the model. For the sake of simplicity, the random interactions and random fields will be treated as independent random variables, even though this does not represent an accurate physical picture, since both randomnesses have a common origin. Our analytical results are valid for arbitrary distributions of random fields, although in the numerical calculations we will restrict ourselves to the Gaussian and bimodal distributions.

### II. THE MODEL

Let us consider a set of Ising spins  $S_i = \pm 1$  located at the sites of two identical sublattices  $A$  and  $B$ , each containing  $N$  sites. The model is defined by the Hamiltonian

$$\mathcal{H} = \sum_{i \in A, j \in B} J_{ij} S_i S_j - \sum_{(ij) \in A} J'_{ij} S_i S_j - \sum_{(ij) \in B} J''_{ij} S_i S_j - \sum_i H_i S_i, \quad (2.1)$$

where the first sum applies to all distinct pairs of spins belonging to different sublattices, the second and third ones refer to all distinct pairs of spins belonging to sublattices  $A$  and  $B$ , respectively, and the last summation is over all spins in the two sublattices. In general, the interactions inside sublattices  $A$  and  $B$  may be distinct, e.g.,  $\{J'_{ij}\}$  and  $\{J''_{ij}\}$ , respectively; herein we shall restrict ourselves to the simplest case where the interactions among pairs of spins belonging either to sublattice  $A$  or  $B$  will be taken from the same probability distribution  $P(J'_{ij})$ . The exchange interactions  $\{J_{ij}\}$  act on pairs of spins of different sublattices, whereas the random

magnetic fields  $\{H_{ij}\}$  act on all sites of the system (both sublattices). The exchange interactions are independent, quenched random variables, following Gaussian probability distributions with mean values

$$\langle J_{ij} \rangle_J = \frac{J_0}{N}, \quad \langle J'_{ij} \rangle_J = \frac{J'_0}{N}, \quad (2.2)$$

and variances

$$\langle J_{ij}^2 \rangle_J - \langle J_{ij} \rangle_J^2 = \frac{J^2}{N}, \quad \langle J'_{ij}{}^2 \rangle_J - \langle J'_{ij} \rangle_J^2 = \frac{J'^2}{N}. \quad (2.3)$$

In the equations above,  $\langle \dots \rangle_J$  represents an average over the corresponding probability distribution of exchange interactions ( $\{J_{ij}\}$  or  $\{J'_{ij}\}$ ). Herein, we assume the mean intrasublattice interactions as ferromagnetic ( $J'_0 > 0$ ) and the mean intersublattice interactions as antiferromagnetic ( $J_0 > 0$ ). The local fields  $\{H_{ij}\}$  are also independent, quenched random variables, identically distributed at each site; their probability distribution will not be specified at this stage.

Following the standard procedure [24,25], we introduce  $n$  replicas  $\alpha = 1, 2, \dots, n$  of the original system and compute the free energy per spin,

$$f = \lim_{n \rightarrow 0} \frac{1}{n} f_n, \quad f_n = \lim_{N \rightarrow \infty} \left( -\frac{1}{2\beta N} \ln \langle \langle Z^n \rangle \rangle_H \right), \quad (2.4)$$

where  $Z^n$  is the partition function of  $n$  copies of the system and  $\beta = 1/k_B T$ . Since the exchange interactions and random fields are independent random variables, their respective averages,  $\langle \dots \rangle_J$  and  $\langle \dots \rangle_H$ , may be performed separately. Averaging  $Z^n$  with respect to the random interactions, one finds

$$\langle Z^n \rangle_J = \text{Tr} \exp \left\{ \beta \left[ \sum_i \sum_\alpha H_i S_i^\alpha - 2N \phi(m_A^\alpha, m_B^\alpha, q_A^{\alpha\beta}, q_B^{\alpha\beta}) \right] \right\}, \quad (2.5)$$

where

$$\begin{aligned} \phi(m_A^\alpha, m_B^\alpha, q_A^{\alpha\beta}, q_B^{\alpha\beta}) &= -\frac{\beta J^2 n}{4} + \frac{J'_0 n}{2N} - \frac{\beta J'^2 n}{4} \left( 1 - \frac{n}{N} \right) + \frac{J_0}{2} \sum_\alpha m_A^\alpha m_B^\alpha \\ &- \frac{J'_0}{4} \sum_\alpha [(m_A^\alpha)^2 + (m_B^\alpha)^2] - \frac{\beta J^2}{2} \sum_{(\alpha\beta)} q_A^{\alpha\beta} q_B^{\alpha\beta} \\ &- \frac{\beta J'^2}{4} \sum_{(\alpha\beta)} [(q_A^{\alpha\beta})^2 + (q_B^{\alpha\beta})^2], \end{aligned} \quad (2.6)$$

and

$$m_{A,B}^\alpha = \frac{1}{N} \sum_{i \in A,B} S_i^\alpha, \quad q_{A,B}^{\alpha\beta} = \frac{1}{N} \sum_{i \in A,B} S_i^\alpha S_i^\beta, \quad (2.7)$$

with  $(\alpha\beta)$  denoting distinct pairs of replicas. In order to transform to a single-site problem, we let the spin variables

$m_{A,B}^\alpha$  and  $q_{A,B}^{\alpha\beta}$  assume continuous values, taking into account the constraints (2.7) by means of the  $\delta$ -function representations,

$$\begin{aligned} &\delta \left( m_{A,B}^\alpha - \frac{1}{N} \sum_{i \in A,B} S_i^\alpha \right) \\ &= \int_{-i\infty}^{i\infty} \frac{Nd\lambda_{A,B}^\alpha}{2\pi i} \\ &\times \exp \left[ -N\lambda_{A,B}^\alpha \left( m_{A,B}^\alpha - \frac{1}{N} \sum_{i \in A,B} S_i^\alpha \right) \right], \\ &\delta \left( q_{A,B}^{\alpha\beta} - \frac{1}{N} \sum_{i \in A,B} S_i^\alpha S_i^\beta \right) \\ &= \int_{-i\infty}^{i\infty} \frac{Nd\lambda_{A,B}^{\alpha\beta}}{2\pi i} \\ &\times \exp \left[ -N\lambda_{A,B}^{\alpha\beta} \left( q_{A,B}^{\alpha\beta} - \frac{1}{N} \sum_{i \in A,B} S_i^\alpha S_i^\beta \right) \right]. \end{aligned} \quad (2.8)$$

The averaging over the random fields leads to

$$\begin{aligned} \langle \langle Z^n \rangle \rangle_H &= \prod_\alpha \int_{-\infty}^{\infty} dm_A^\alpha \int_{-\infty}^{\infty} \frac{Nd\lambda_A^\alpha}{2\pi i} \int_{-\infty}^{\infty} dm_B^\alpha \\ &\times \int_{-\infty}^{\infty} \frac{Nd\lambda_B^\alpha}{2\pi i} \prod_{(\alpha\beta)} \int_{-\infty}^{\infty} dq_A^{\alpha\beta} \int_{-\infty}^{\infty} \frac{Nd\lambda_A^{\alpha\beta}}{2\pi i} \\ &\times \int_{-\infty}^{\infty} dq_B^{\alpha\beta} \int_{-\infty}^{\infty} \frac{Nd\lambda_B^{\alpha\beta}}{2\pi i} \exp[-2N\beta f_n \\ &\times (m_A^\alpha, m_B^\alpha, q_A^{\alpha\beta}, q_B^{\alpha\beta}; \lambda_A^\alpha, \lambda_B^\alpha, \lambda_A^{\alpha\beta}, \lambda_B^{\alpha\beta})], \end{aligned} \quad (2.9)$$

where, after dropping out the site index notation,

$$\begin{aligned} f_n &= \phi(m_A^\alpha, m_B^\alpha, q_A^{\alpha\beta}, q_B^{\alpha\beta}) + \frac{1}{2\beta} \sum_\alpha (\lambda_A^\alpha m_A^\alpha + \lambda_B^\alpha m_B^\alpha) \\ &+ \frac{1}{2\beta} \sum_{(\alpha\beta)} (\lambda_A^{\alpha\beta} q_A^{\alpha\beta} + \lambda_B^{\alpha\beta} q_B^{\alpha\beta}) - \frac{1}{2\beta} \ln \langle \text{Tr} \exp \bar{\mathcal{H}}_A \rangle_H \\ &- \frac{1}{2\beta} \ln \langle \text{Tr} \exp \bar{\mathcal{H}}_B \rangle_H, \end{aligned} \quad (2.10)$$

with  $\bar{\mathcal{H}}_{A,B}$  denoting the ‘‘effective sublattice Hamiltonians,’’ given by

$$\bar{\mathcal{H}}_{A,B} = \sum_\alpha (\beta H + \lambda_{A,B}^\alpha) S^\alpha + \sum_{(\alpha\beta)} \lambda_{A,B}^{\alpha\beta} S^\alpha S^\beta. \quad (2.11)$$

In the thermodynamic limit  $N \rightarrow \infty$ , the integrations over the  $\lambda$  variables may be performed by the saddle-point method; the saddle-point equations are given by

$$m_{A,B}^\alpha = \frac{\langle \text{Tr} S^\alpha \exp \tilde{\mathcal{H}}_{A,B} \rangle_H}{\langle \text{Tr} \exp \tilde{\mathcal{H}}_{A,B} \rangle_H}, \quad q_{A,B}^{\alpha\beta} = \frac{\langle \text{Tr} S^\alpha S^\beta \exp \tilde{\mathcal{H}}_{A,B} \rangle_H}{\langle \text{Tr} \exp \tilde{\mathcal{H}}_{A,B} \rangle_H}. \quad (2.12)$$

The above equations allows one to determine the  $\lambda$  variables in terms of the  $m$  and  $q$  variables; performing the integrations over the  $m$  and  $q$  variables by the Laplace method, one finds that the condition for  $f_n$  to be stationary with respect to such variables yields

$$\lambda_{A,B}^\alpha = \beta J'_0 m_{A,B}^\alpha - \beta J_0 m_{B,A}^\alpha, \quad \lambda_{A,B}^{\alpha\beta} = \beta^2 J'^2 q_{A,B}^{\alpha\beta} + \beta^2 J^2 q_{B,A}^{\alpha\beta}. \quad (2.13)$$

Substituting the results above into Eq. (2.10),

$$\begin{aligned} f_n = & -\frac{\beta}{4}(J^2 + J'^2)n - \frac{J_0}{2} \sum_{\alpha} m_A^\alpha m_B^\alpha + \frac{J'_0}{4} \\ & \times \sum_{\alpha} [(m_A^\alpha)^2 + (m_B^\alpha)^2] + \frac{\beta J^2}{2} \sum_{(\alpha\beta)} q_A^{\alpha\beta} q_B^{\alpha\beta} + \frac{\beta J'^2}{4} \\ & \times \sum_{(\alpha\beta)} [(q_A^{\alpha\beta})^2 + (q_B^{\alpha\beta})^2] - \frac{1}{2\beta} \ln \langle \text{Tr} \exp \tilde{\mathcal{H}}_A \rangle_H \\ & - \frac{1}{2\beta} \ln \langle \text{Tr} \exp \tilde{\mathcal{H}}_B \rangle_H, \end{aligned} \quad (2.14)$$

where we have discarded terms that vanish in the limit  $N \rightarrow \infty$ . Analogously, the effective sublattice Hamiltonians in Eq. (2.11) become

$$\begin{aligned} \tilde{\mathcal{H}}_{A,B} = & \sum_{\alpha} (\beta H + \beta J'_0 m_{A,B}^\alpha - \beta J_0 m_{B,A}^\alpha) S^\alpha + \sum_{(\alpha\beta)} (\beta^2 J'^2 q_{A,B}^{\alpha\beta} \\ & + \beta^2 J^2 q_{B,A}^{\alpha\beta}) S^\alpha S^\beta. \end{aligned} \quad (2.15)$$

In the next section we will consider a simple choice for the parameters  $m_{A,B}^\alpha$  and  $q_{A,B}^{\alpha\beta}$ , the so-called replica-symmetric solution.

### III. THE REPLICA-SYMMETRIC SOLUTION

The replica-symmetric (RS) solution is obtained by assuming order parameters independent of replica indices,

$$m_{A,B}^\alpha = m_{A,B} \quad (\forall \alpha), \quad q_{A,B}^{\alpha\beta} = q_{A,B} \quad [\forall (\alpha\beta)]. \quad (3.1)$$

Proceeding in the usual way, one finds that the stationary conditions (2.12) and (2.13) yield the equations of state

$$m_{A,B} = \langle \langle \tanh \Phi_{A,B} \rangle \rangle_H, \quad q_{A,B} = \langle \langle \tanh^2 \Phi_{A,B} \rangle \rangle_H, \quad (3.2)$$

where

$$\Phi_{A,B} = \beta(H + J'_0 m_{A,B} - J_0 m_{B,A} + \sqrt{J'^2 q_{A,B} + J^2 q_{B,A}^x}), \quad (3.3)$$

and the brackets without subscript  $\langle \dots \rangle$  denote Gaussian averages,

$$\langle \dots \rangle = \int_{-\infty}^{\infty} \frac{dx}{\sqrt{2\pi}} e^{-x^2/2} (\dots). \quad (3.4)$$

In the same way, the free energy per spin in Eq. (2.4) becomes

$$\begin{aligned} f = & -\frac{\beta J^2}{4}(1-q_A)(1-q_B) - \frac{\beta J'^2}{8}[(1-q_A)^2 + (1-q_B)^2] \\ & - \frac{J_0}{2} m_A m_B + \frac{J'_0}{4}(m_A^2 + m_B^2) - \frac{1}{2\beta} \langle \langle \ln 2 \cosh \Phi_A \rangle \rangle_H \\ & - \frac{1}{2\beta} \langle \langle \ln 2 \cosh \Phi_B \rangle \rangle_H. \end{aligned} \quad (3.5)$$

To determine the validity of the RS solution it is necessary to study its stability against fluctuations in the replica space [12]. Such analysis of stability is similar to the one of the antiferromagnetic spin glass without random fields [7,9,10]. One finds that the RS solution becomes unstable against ‘‘transversal’’ fluctuations, i.e., fluctuations outside the replica-symmetric space, when one of the following de Almeida-Thouless (AT) stability conditions is violated,

$$2 - \beta^2 J'^2(1-2q_A+r_A) - \beta^2 J'^2(1-2q_B+r_B) > 0, \quad (3.6)$$

$$\begin{aligned} [1 - \beta^2 J'^2(1-2q_A+r_A)][1 - \beta^2 J'^2(1-2q_B+r_B)] \\ - \beta^4 J^4(1-2q_A+r_A)(1-2q_B+r_B) > 0, \end{aligned} \quad (3.7)$$

where

$$r_{A,B} = \langle \langle \tanh^4 \Phi_{A,B} \rangle \rangle_H. \quad (3.8)$$

The ‘‘transversal’’ instability of the RS solution is usually associated with the necessity of a replica-symmetry-breaking (RSB) procedure [13,14] and the emergence of a spin-glass phase. An RS solution will be called stable if it satisfies the conditions (3.6) and (3.7), and unstable otherwise.

We will now discuss the thermodynamic behavior of the system within the RS approach. In our numerical calculations we found that different types of solutions of the set of equations (3.2) are possible, depending on the values of the various parameters of the model. In the absence of uniform or random fields, we can distinguish the *paramagnetic* ( $P$ ) solution ( $q_A = q_B = 0$ ,  $m_A = m_B = 0$ ), the *spin-glass* (SG) solution ( $q_A = q_B > 0$ ,  $m_A = m_B = 0$ ), and the *antiferromagnetic* (AF) solution ( $q_A = q_B > 0$ ,  $m_A = -m_B$ ). An unstable AF solution will be called *mixed antiferromagnetic* (AF'). The presence of uniform or random fields always induces the spin-glass order parameter, and we can distinguish only the ‘‘saturated’’ *paramagnetic* ( $P$ ) solution ( $q_A = q_B > 0$ ,  $m_A = m_B$ ), and the *antiferromagnetic* (AF) solution ( $q_A > 0$ ,  $q_B > 0$ ,  $m_A \neq m_B$ ). In this case, the unstable  $P$  solution will be called spin glass (SG) and the unstable AF solution will be called mixed antiferromagnetic (AF'). A detailed discussion of these nomenclatures will be given in some specific examples in the next section. We observe that the SG and AF' solutions are unstable, and the correct solutions would require the consideration of RSB procedures, which are beyond the purpose of this work. If there are two unstable RS solutions, it is not possible to choose one of them solely from considerations of stability. In such cases we choose the solution that seems more plausible from the physical point of view, even though it may imply a higher free energy. We

believe that a correct choice could in principle be made by studying the stability against ‘‘longitudinal’’ fluctuations, i.e., fluctuations within the replica-symmetric space. In the case of the standard SK model, such study leads to the conclusion that the RS free energy should be a maximum with respect to the spin-glass order parameter [24,25]. However, in the present work we limit ourselves to the consideration of stability against ‘‘transversal’’ fluctuations. In cases where there are both stable and unstable solutions, we always choose the stable one. Finally, when there are two or more stable solutions, we choose the one with the lowest free energy. The first-order transition is determined numerically by equalizing the free energies. However, it is possible to obtain some analytic results for the critical lines and tricritical points.

Let us begin with the simplest case of a symmetric random-field distribution obeying  $P(H)=P(-H)$ . In this case, one may easily see that

$$m_A = -m_B = m, \quad q_A = q_B = q. \quad (3.9)$$

Therefore, the set of equations (3.2) become

$$m = \langle \langle \tanh \Phi \rangle \rangle_H, \quad q = \langle \langle \tanh^2 \Phi \rangle \rangle_H, \quad (3.10)$$

with

$$\Phi = \beta[H + (J'_0 + J_0)m + \sqrt{(J'^2 + J^2)qx}]. \quad (3.11)$$

Also, the stability conditions (3.6) and (3.7) reduce to

$$1 - \beta^2(J'^2 + J^2)(1 - 2q + r) > 0 \quad (3.12)$$

where

$$r = \langle \langle \tanh^4 \Phi \rangle \rangle_H. \quad (3.13)$$

In the absence of random fields, the above equations recover those of the conventional SK model [6,12] in zero magnetic field and exchange interactions with mean  $(J'_0 + J_0)/N$  and variance  $(J'^2 + J^2)/N$ . Therefore, the phase diagrams are similar, except for the fact that the ferromagnetic phase should be replaced by an antiferromagnetic phase. In the presence of random fields, the transition from the paramagnetic phase ( $m=0$ ) to the antiferromagnetic phase ( $m \neq 0$ ) may be found by expanding equations (3.10) in powers of the sublattice magnetization  $m$ . After some calculations one finds

$$m = am + bm^3 + cm^5 + \dots, \quad (3.14)$$

where

$$a = \beta(J_0 + J'_0)(1 - q), \quad (3.15)$$

$$b = -\frac{1}{3}\beta^3(J_0 + J'_0)^3(1 - 4q + 3r) \\ \times \left[ \frac{1 + 2\beta^2(J^2 + J'^2)(1 - 4q + 3r)}{1 - \beta^2(J^2 + J'^2)(1 - 4q + 3r)} \right], \quad (3.16)$$

and we have omitted the rather lengthy expression for the  $c$  coefficient. In the above equations  $q$  and  $r$  correspond to the

paramagnetic solution ( $m=0$ ) determined from Eqs. (3.10) and (3.13). There is only the paramagnetic phase if  $a < 1$ ,  $b < 0$ , and  $c < 0$ , and a second-order transition to the antiferromagnetic phase takes place for  $a = 1$  and  $b, c < 0$ . A tricritical point occurs if  $a = 1$ ,  $b = 0$ , and  $c < 0$ . If one considers no intrasublattice interactions ( $J'_0 = J'_0 = 0$ ), Eqs. (3.15) and (3.16) recover those of the ferromagnetic SK model in the presence of random fields following symmetric distributions (Gaussian [26,27] and bimodal [28]).

For nonsymmetric distributions of random fields, it is necessary to analyze the whole set of four equations (3.2). The transition from the paramagnetic to the antiferromagnetic phase should be characterized by the onset of the staggered magnetization [11],

$$m_s = \frac{m_A - m_B}{2}. \quad (3.17)$$

After rather laborious calculations one finds the expansion

$$m_s = am_s + bm_s^3 + cm_s^5 + \dots, \quad (3.18)$$

where

$$a = \beta(J_0 + J'_0) \left[ (1 - q) - \frac{2\beta^2(J'^2 - J^2)(m - t)^2}{1 - \beta^2(J'^2 - J^2)(1 - 4q + 3r)} \right], \quad (3.19)$$

and we shall omit the  $b$  coefficient which is already very lengthy. In the equation above the parameters  $m$ ,  $q$ ,  $t$ , and  $r$  correspond to the paramagnetic solution  $m_A = m_B = m$  and  $q_A = q_B = q$ , being given by

$$m = \langle \langle \tanh \Phi \rangle \rangle_H, \quad q = \langle \langle \tanh^2 \Phi \rangle \rangle_H, \quad (3.20)$$

$$t = \langle \langle \tanh^3 \Phi \rangle \rangle_H, \quad r = \langle \langle \tanh^4 \Phi \rangle \rangle_H, \quad (3.21)$$

with

$$\Phi = \beta[H + (J'_0 - J_0)m + \sqrt{(J'^2 + J^2)qx}]. \quad (3.22)$$

It is important to notice that for the particular case of a symmetric random field distribution,  $m = t = 0$ , in such a way that the coefficient of Eq. (3.19) reduces to the one of Eq. (3.15), as it should. There is only the paramagnetic phase if  $a < 1$  and  $b < 0$ ; a second-order transition from paramagnetic to the antiferromagnetic phase takes place for  $a = 1$  and  $b < 0$ . Tricritical points may occur if  $a = 1$ ,  $b = 0$ , and  $c < 0$ ; however, since we did not compute the  $c$  coefficient, we cannot check the condition  $c < 0$ , and other possibilities such as critical and bicritical endpoints [11] cannot be ruled out. In the limit of zero variance of the random-field distribution, the results above reduce to those already obtained for the case of an antiferromagnetic spin glass [9].

In the next section we present the results obtained from a numerical analysis of the equations derived above.

#### IV. NUMERICAL RESULTS

Let us now consider two particular choices of random fields, specified, respectively, by the Gaussian and bimodal probability distributions. In the numerical analysis which fol-

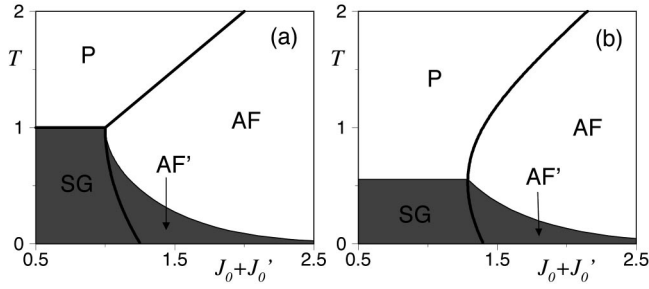


FIG. 1. Phase diagrams for the antiferromagnetic spin glass in the presence of random fields, for a symmetric random-field Gaussian distribution with (a)  $\sigma=0$  and (b)  $\sigma=0.5$ . The heavy lines indicate continuous transitions. Throughout the shaded regions the RS solution is unstable. The several phases are paramagnetic ( $P$ ), antiferromagnetic ( $AF$ ), spin glass ( $SG$ ), and mixed antiferromagnetic ( $AF'$ ), as defined in the text. Our temperature and energy units are such that  $k_B=1$  and  $\sqrt{J^2+J'^2}=1$ .

lows, we work in temperature and energy units in such a way that

$$k_B=1, \quad \sqrt{J^2+J'^2}=1. \quad (4.1)$$

### A. Gaussian distribution

We consider a Gaussian distribution for the random fields, with mean  $H_0$  and variance  $\sigma^2$ ,

$$P(H) = \frac{1}{\sqrt{2\pi}\sigma} \exp\left[-\frac{1}{2\sigma^2}(H-H_0)^2\right]. \quad (4.2)$$

The average of any function  $g$  of the effective fields  $\Phi_{A,B}$ , with respect to the Gaussian random field, can be easily performed; one gets

$$\langle\langle g(\Phi_{A,B}) \rangle\rangle_H = \langle g(\Phi'_{A,B}) \rangle, \quad (4.3)$$

where

$$\Phi'_{A,B} = \beta(H_0 + J'_0 m_{A,B} - J_0 m_{B,A} + \sqrt{J'^2 q_{A,B} + J^2 q_{B,A} + \sigma^2} x). \quad (4.4)$$

Let us first consider the case of a symmetric random-field distribution, i.e.,  $H_0=0$ . As discussed in the previous section, for  $\sigma=0$  the phase diagram is identical to the one of the conventional SK model [6], with the ferromagnetic phase replaced by an antiferromagnetic phase, as shown in Fig. 1(a). For  $\sigma>0$  the transition from the paramagnetic to the antiferromagnetic phase is determined by the condition  $a=1$  given by Eq. (3.15). This transition is continuous for all  $\sigma>0$ , since the coefficient  $b$  given by Eq. (3.16) is always negative for  $a=1$ . The phase diagram for a typical choice of random-field variance  $\sigma=0.5$  is exhibited in Fig. 1(b). Our results are in agreement with previous work on the SK model in the presence of a random-field following a symmetric Gaussian distribution [27]. One notices that as the field randomness (i.e., the variance  $\sigma^2$ ) increases, the paramagnetic phase becomes dominant, pushing the antiferromagnetic phases ( $AF$  and  $AF'$ ) to the region of increasing  $J_0+J'_0$ , while depressing the spin-glass phase to the low-temperature region. Thus, the antiferromagnetic phases will be destroyed

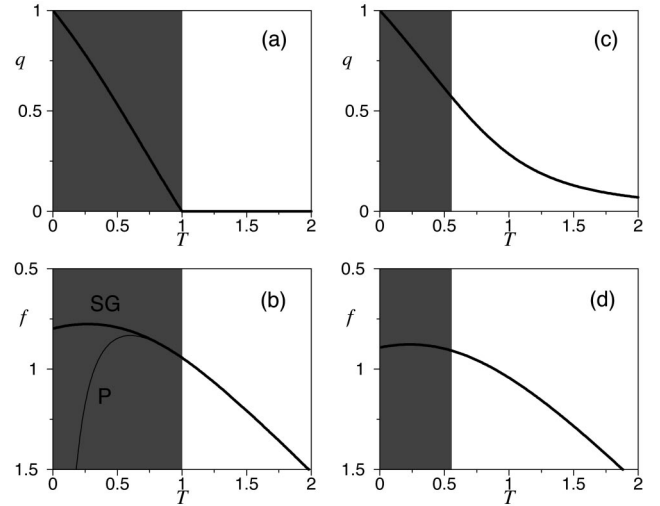


FIG. 2. The spin-glass order parameter  $q$  and the free-energy per spin  $f$ , as a function of the temperature, for the fixed value  $J_0+J'_0=0.5$  in the phase diagrams of Fig. 1. In (a) and (b), corresponding to  $\sigma=0$ , a continuous  $P$ - $SG$  phase transition occurs at  $T=1$ ; at low temperatures the  $SG$  solution leads to a higher free energy (heavy line) than the analytic continuation of the  $P$  solution (thin line). In (c) and (d), the field randomness  $\sigma=0.5$  induces the spin-glass order parameter in such a way that no  $P$ - $SG$  phase transition occurs within the replica-symmetry approximation. In the shaded regions the RS solution is unstable.

by a random field with large enough  $\sigma$ , whereas the spin-glass phase will always survive, even though at very low temperatures.

In Fig. 2 we exhibit the spin-glass order parameter  $q$  and the free-energy per spin  $f$ , as a function of the temperature, for the fixed value  $J_0+J'_0=0.5$  in the phase diagrams of Figs. 1(a) and 1(b), corresponding to  $\sigma=0$  and  $\sigma=0.5$ , respectively. We observe that the magnetizations are identically zero for all temperatures ( $m_A=m_B=0$ ). In the case  $\sigma=0$  the result is identical to the standard SK model. Below the temperature  $T=1$  there are two solutions: paramagnetic ( $q=0$ ) and spin glass ( $q>0$ ) [see Fig. 2(a)]. As is well known [24,25], the analytic continuation of the paramagnetic solution down to low temperatures leads to a lower free energy than the one of the spin-glass solution [see Fig. 2(b)], but the paramagnetic solution is unacceptable because it is not stable. Although the RS spin-glass solution is also unstable, it is believed that the correct RSB spin-glass solution would be stable [24,25]. In the case  $\sigma=0.5$  the spin-glass order parameter  $q$  is always induced by the random field and there is only one solution  $q>0$  for all temperatures, as shown in Fig. 2(c), with the free energy presenting a simple behavior with the temperature [see Fig. 2(d)]. At high temperatures this solution should correspond to the paramagnetic phase. However, below  $T=0.55548$  the solution ceases to be stable. In analogy to what happens for the SK model in the presence of a uniform magnetic field, where the low-temperature region of a paramagnetic phase (below the AT line) is sometimes referred to as a spin-glass phase [24,25], we shall adopt herein the same nomenclature for the low-temperature regions of our paramagnetic phases, where the AT instability gets manifested.

In Fig. 3 we exhibit the magnetizations and spin-glass

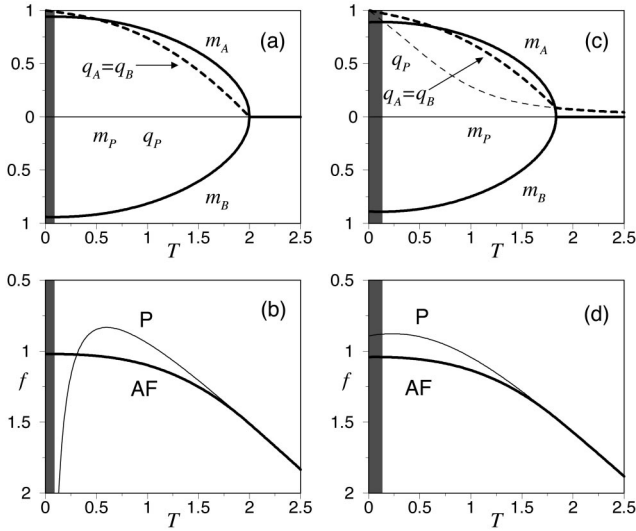


FIG. 3. The magnetizations and spin-glass order parameters, as well as the free energy per spin, as a function of the temperature, for the fixed value  $J_0 + J'_0 = 2$  in the phase diagrams of Fig. 1. (a) and (b) correspond to field randomness  $\sigma = 0$  and (c) and (d) to  $\sigma = 0.5$ . In (a) and (c), the heavy full lines represent the sublattice magnetizations  $m_A$  and  $m_B$ , whereas the heavy dashed lines refer to the sublattice spin-glass parameters  $q_A$  and  $q_B$ ; the full and dashed thin lines represent, respectively, the paramagnetic solutions  $m_P$  and  $q_P$ . In (b) and (d), the heavy and thin lines represent, respectively, the free energies associated with the AF and  $P$  solutions. Throughout the shaded regions the RS AF solution is unstable.

order parameters, as well as the free-energy per spin, as a function of the temperature, for the fixed value  $J_0 + J'_0 = 2$  in the phase diagrams of Figs. 1(a) and 1(b), corresponding to  $\sigma = 0$  and  $\sigma = 0.5$ , respectively. In the case  $\sigma = 0$ , for temperatures  $T > 2$  there is only the paramagnetic solution,  $m = 0$  and  $q = 0$ , whereas below  $T = 2$  there is also the possibility of the antiferromagnetic solution,  $q_A = q_B > 0$  and  $m_A = -m_B$ , as shown in Fig. 3(a). The free energy of the AF solution is lower throughout most of the temperature range  $T < 2$ , although the unstable  $P$  solution yields a lower free energy as  $T \rightarrow 0$  [see Fig. 3(b)]. The AF solution ceases to be stable at a temperature  $T = 0.089482$ . The part of the AF phase where such an instability occurs will be called a mixed phase, characterized by both antiferromagnetic ordering and replica-symmetry instability, in analogy with the mixed phase of the standard SK model [24,25]. In the case of  $\sigma = 0.5$ , the field randomness induces the spin-glass order parameter even for the paramagnetic solution [see Fig. 3(c)]. In this case the free energy of the AF solution is always lower than the  $P$  solution, as exhibited in Fig. 3(d). The AF solution becomes unstable at a temperature  $T = 0.13201$ , below which there is the mixed AF phase.

We now consider the effects of nonzero averages for the random fields ( $H_0 > 0$ ). Unlike the ferromagnetic phase of the SK model in a random field [27], the antiferromagnetic phase that exists for  $H_0 = 0$  will survive up to a certain value of  $H_0$ . In the case of zero field disorder ( $\sigma = 0$ ), it has been found that the phase diagram in the  $T - H_0$  plane may exhibit either a continuous transition line [7,8], or one (or two) tricritical points separating a first-order transition line from continuous transition lines [9]. An exhaustive study of all

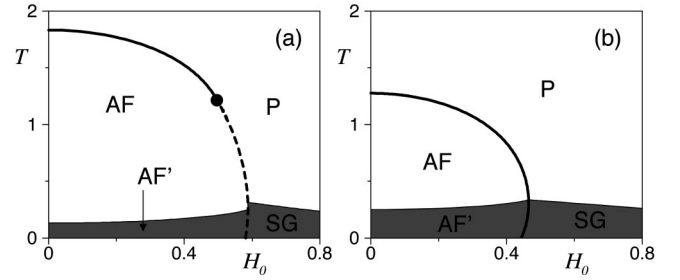


FIG. 4. Phase diagrams of the antiferromagnetic spin glass in the presence of random fields following a nonsymmetric Gaussian distribution for  $J'/J = 1$ ,  $J'_0/J_0 = 2$ , and  $J_0 + J'_0 = 2$ , with field randomnesses (a)  $\sigma = 0.5$  and (b)  $\sigma = 1$ . The heavy solid and dashed lines represent, respectively, continuous and first-order transitions. In (a) these lines meet at a tricritical point represented by a black circle. The thin lines delimit shaded regions where the RS solution is unstable, indicating the onset of the spin-glass and mixed-antiferromagnetic phases; one notices that in (a) such lines present a gap across the first-order transition. Our units and phase nomenclature are as defined in Fig. 1.

possibilities becomes difficult because the phase diagrams depend on four parameters ( $J'/J$ ,  $J'_0/J_0$ ,  $J_0 + J'_0$ , and  $\sigma$ ). In order to illustrate the effects of Gaussian random fields, we shall consider the case  $J'/J = 1$ ,  $J'_0/J_0 = 2$ , and  $J_0 + J'_0 = 2$ . The results of our numerical analysis are summarized in Fig. 4 for typical values of  $\sigma$ . The continuous transition lines were determined from the condition  $a = 1, b < 0$ , where the coefficient  $a$  is given by Eq. (3.19). The tricritical points correspond to  $a = 1, b = 0$ , and below them, the first-order transition lines were determined equating the free energies of the paramagnetic and antiferromagnetic phases. This procedure is illustrated in Fig. 5, corresponding to one particular choice of temperature in Fig. 4(a). By fixing the temperature in  $T = 0.5$ , and varying the average value of the Gaussian random field  $H_0$ , a first-order phase transition occurs for  $H_0 = 0.58162$ . In the vicinity of the first-order phase transition there are more than one solution for the order parameters [Figs. 5(a) and 5(b)]; we choose the ones which correspond to a minimum of the free energy [Figs. 5(c) and 5(d)]. In Fig. 4 we also exhibit the lines below which the AT stability conditions (3.6) and (3.7) are violated, signaling the onset of the spin-glass and mixed-antiferromagnetic phases. Due to discontinuities in the order parameters [see Figs. 5(a) and 5(b)], whenever the RS instabilities occur within first-order transitions, they do not meet across the first-order transition line, i.e., one finds a jump in the AT line separating phases  $P$ -SG with respect to the one separating phases AF-AF'. Similar jumps in the AT lines have also been found for the antiferromagnetic SK model in the presence of a uniform magnetic field [9], as well as for the ferromagnetic SK model under random fields following a symmetric bimodal probability distribution [28]. For small field randomness, e.g.,  $\sigma = 0.5$  shown in Fig. 4(a), the phase diagram displays an antiferromagnetic phase separated from a paramagnetic phase by a continuous line, at high temperatures, and a first-order transition line, at low temperatures, with such lines meeting at a tricritical point; the transitions to the spin-glass and mixed-antiferromagnetic phases are discontinuous across the first-order transition line. These results are in agreement with

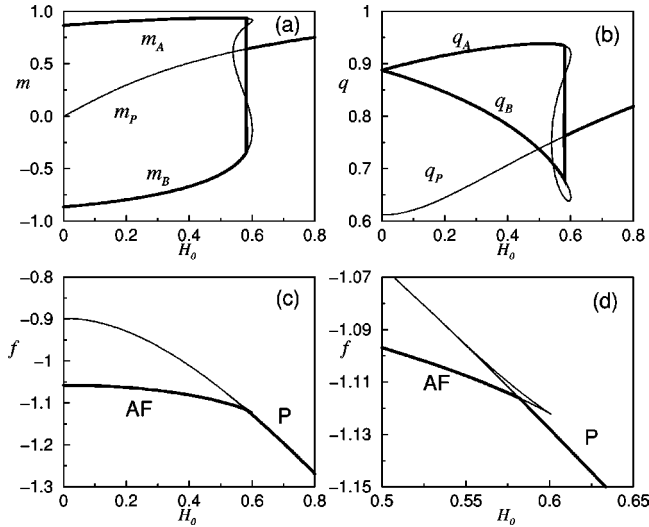


FIG. 5. The magnetizations and spin-glass order parameters, as well as the free energy per spin, as a function of the average of the random field, for a fixed value of the temperature,  $T=0.5$ , in the phase diagram of Fig. 4(a) corresponding to  $\sigma=0.5$ . A first-order phase transition occurs at  $H_0=0.58162$ . In (a)  $m_A$  and  $m_B$  denote the sublattice magnetizations of the AF solution, whereas  $m_P$  represents the one of the  $P$  solution. In (b),  $q_A$  and  $q_B$  refer to the AF sublattice spin-glass order parameters, whereas  $q_P$  refers to the one of the  $P$  solution. The corresponding free energy is shown in (c) and the detail in the vicinity of the first-order phase transition is exhibited in (d). The heavy line depicts the solution with the lowest free energy. We observe that for this temperature the RS solution is always stable.

previous works on antiferromagnetic spin glasses in the presence of a uniform magnetic field [9,10]. The effects of increasing field randomness is to weaken the first-order transition, to decrease the antiferromagnetic phases, while enlarging the paramagnetic and spin-glass phases. For a sufficiently high field randomness, e.g.,  $\sigma=1$  shown in Fig. 4(b), the first-order transition disappears completely. By increasing further the field randomness, one notices that the antiferromagnetic phases may get totally destroyed.

### B. Bimodal distribution

We now consider the random field obeying a bimodal, or double- $\delta$  distribution,

$$P(H) = \frac{1}{2} \delta(H - H_0 + \sigma) + \frac{1}{2} \delta(H - H_0 - \sigma). \quad (4.5)$$

The average of any function  $g$  of the effective fields  $\Phi_{A,B}$ , with respect to the bimodal random field is, given straightforwardly by

$$\langle\langle g(\Phi_{A,B}) \rangle\rangle_H = \frac{1}{2} \langle g(\Phi_{A,B}^+) \rangle + \frac{1}{2} \langle g(\Phi_{A,B}^-) \rangle, \quad (4.6)$$

where

$$\Phi_{A,B}^\pm = \beta(H_0 \pm \sigma + J'_0 m_{A,B} - J_0 m_{B,A} + \sqrt{J'^2 q_{A,B} + J^2 q_{B,A} x}). \quad (4.7)$$

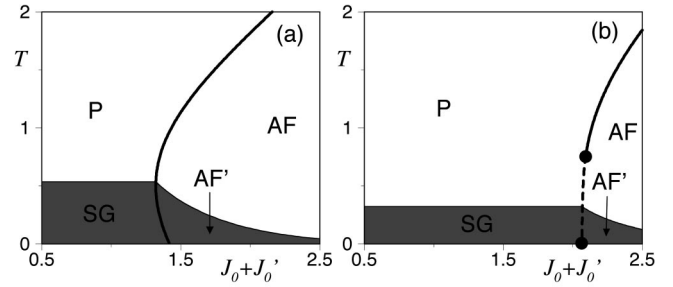


FIG. 6. Phase diagrams for a symmetric bimodal random-field distribution with (a)  $\sigma=0.5$  and (b)  $\sigma=1$ . The heavy solid and dashed lines represent, respectively, continuous and first-order transitions. In (b) there are two tricritical points indicated by black circles, the lower one occurring at  $T=0$ . The thin lines delimit the shaded region where the RS solution is unstable, indicating the onset of the spin-glass and mixed-antiferromagnetic phases. Our units and phase nomenclature are as defined in Fig. 1.

We observe that the numerical study of the bimodal case is very similar to the Gaussian one, simply using the expression for the average in Eq. (4.6) instead of the one in Eq. (4.3). One should also notice that in the absence of field randomness ( $\sigma=0$ ), the bimodal and Gaussian cases coincide, both recovering the antiferromagnetic spin glass, already studied in the literature [7–10].

Let us first consider the case  $H_0=0$ , i.e., a symmetric random-field distribution. The phase diagram in this case can be inferred from previous work on the ferromagnetic SK model in a random field following a symmetric bimodal distribution [28], simply replacing the ferromagnetic phase by an antiferromagnetic phase. The main difference between the bimodal and the Gaussian cases is that for  $\sigma>0.9573$  the critical frontier separating the paramagnetic and antiferromagnetic phases may be of first order. For  $0.9573<\sigma<1$ , as the temperature is lowered, the continuous critical frontier changes to a first-order transition line at a tricritical point; as the temperature is further lowered, the first-order critical frontier changes again to a continuous line at a second tricritical point. However for  $\sigma>1$  the first-order transition line extends down to  $T=0$  and only one tricritical point remains [28]. Results for  $\sigma=0.5$  and  $\sigma=1$  are presented in Fig. 6. It is important to notice that for  $\sigma=1$  there are two tricritical points, the second one occurring at  $T=0$ . Also shown in Fig. 6 are the lines below which the AT stability condition (3.12) is violated, signaling the onset of the spin-glass and mixed-antiferromagnetic phases.

Let us now consider a nonsymmetric bimodal distribution, i.e.,  $H_0>0$ . The antiferromagnetic phase that exists in  $H_0=0$  will always survive up to a certain value of  $H_0$ . To illustrate the effects of the bimodal random field, we choose the same parameters used in the Gaussian case, i.e.,  $J'/J=1$ ,  $J'_0/J_0=2$ , and  $J_0+J'_0=2$ . The results of our numerical analysis, for  $\sigma=0.5$  and  $\sigma=0.9$ , are presented in Fig. 7. It is important to mention that for  $\sigma=1$ , unlike in the Gaussian case, the antiferromagnetic phase is completely destroyed by the random field. It is clear from Fig. 7 that the effects of bimodal random fields do not differ qualitatively from those of Gaussian random fields, at least for the choice of parameters considered herein.

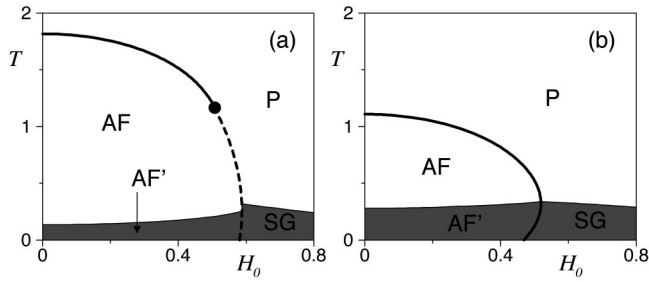


FIG. 7. Phase diagrams of the antiferromagnetic spin glass in the presence of random fields following a nonsymmetric bimodal distribution for  $J'/J=1$ ,  $J'_0/J_0=2$ , and  $J_0+J'_0=2$ , with field randomnesses (a)  $\sigma=0.5$  and (b)  $\sigma=0.9$ . The heavy solid and dashed lines represent, respectively, continuous and first-order transitions. In (a) these lines meet at a tricritical point represented by a black circle. The thin lines delimit shaded regions where the RS solution is unstable, indicating the onset of the spin-glass and mixed-antiferromagnetic phases; one notices that in (a) such lines present a gap across the first-order transition. Our units and phase nomenclature are as defined in Fig. 1.

## V. DISCUSSIONS

According to our calculations, the main effect of the random field in antiferromagnetic spin glasses is to decrease the extensions of the antiferromagnetic phases; in the cases where there is a first-order transition line, the introduction of a random field also decreases the extension of such a line. For a sufficiently large field randomness, first-order transitions are converted into continuous ones, whereas for a still larger randomness, the antiferromagnetic phases disappear. The destruction of the first-order transition line in  $\text{Fe}_x\text{Mg}_{1-x}\text{Cl}_2$ , due to random fields, was observed recently [29].

For a specific application of our results, let us consider the effect of the Gaussian random field for the case  $J'/J=J'_0/J_0=5$  and  $J_0+J'_0=1.1$ , which is appropriate to describe  $\text{Fe}_x\text{Mn}_{1-x}\text{TiO}_3$  [10]. In the absence of the random field ( $\sigma=0$ ), there is a first-order transition line meeting continuous lines at two tricritical points, as shown in Fig. 8(a). Actually, we found numerically that such lines do not meet smoothly at the putative tricritical point at higher temperatures (in a region where the RS solution adopted herein is stable), determined by the conditions  $a=1, b=0$  [with  $a$  given by Eq. (3.19)]. This suggests the occurrence of critical and bicritical endpoints [11], instead of a tricritical point. Also shown are the lines beyond which the AT stability conditions (3.6) and (3.7) are violated, signaling the onset of the spin-glass and mixed-antiferromagnetic phases. Our results for  $\sigma=0$  are in good agreement with previous calculations [10] using the same parameter values (for a better comparison with the results of Takayama, in Fig. 8 we have inverted the axes with respect to those of Figs. 4 and 7). With the application of a random field with  $\sigma=0.15$ , the first-order transition is converted into a continuous line, while the antiferromagnetic phases decrease in size, as shown in Fig. 8(b). Thus, the inclusion of a random field makes the theoretical

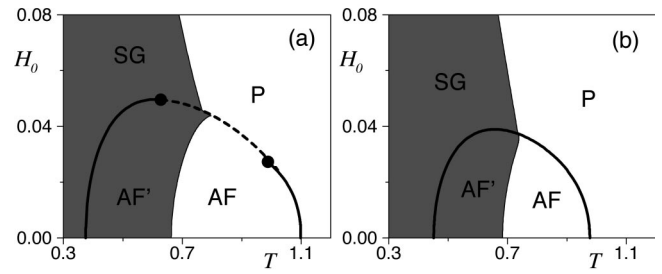


FIG. 8. Phase diagrams of the antiferromagnetic spin glass in the presence of random fields following a nonsymmetric Gaussian distribution for  $J'/J=J'_0/J_0=5$ ,  $J_0+J'_0=1.1$ , with field randomnesses (a)  $\sigma=0$  and (b)  $\sigma=0.15$ . The heavy solid and dashed lines represent, respectively, continuous and first-order transitions. In (a) these lines meet at tricritical points represented by black circles (notice that, at high temperatures, such lines do not meet smoothly). The thin lines delimit regions where the RS solution is unstable, indicating the onset of the spin-glass and mixed-antiferromagnetic phases. Our units and phase nomenclature are as defined in Fig. 1.

calculations match more closely the experimental results, in which no first-order transition is detected [15]. However, it is possible that the first-order transition may also be eliminated without the inclusion of random fields, by slightly changing the parameter values  $J'/J$ ,  $J'_0/J_0$ , or  $J_0+J'_0$  [9].

It should be mentioned that all the results presented above were obtained within the simplest choice for the order parameters, i.e., the RS solution. Although such a solution is valid at high temperatures, it becomes unstable at low temperatures (below the AT lines drawn in our phase diagrams). Important low-temperature effects, like phase reentrances and tricritical points, inside such a region, may change completely under a more appropriate choice for the order parameters [13,14].

We emphasize that there are important experimental observations not captured by our calculations. Experimental works in the mixed antiferromagnetic compound  $\text{Fe}_x\text{Mn}_{1-x}\text{TiO}_3$  [15] and in the diluted antiferromagnet  $\text{Fe}_x\text{Zn}_{1-x}\text{F}_2$  [19,22,23] have reported two irreversibility phenomena, a weak one at higher temperatures, attributed to the random-field effect, and a stronger one at lower temperatures, attributed to the spin-glass ordering. Since the mean-field theory of the ferromagnetic random-field Ising model [30,31] does not indicate any kind of glassy phase induced by the random field, it is natural to expect the same limitation in our mean-field calculations. Presumably, a much more sophisticated approach [32–34] is needed to describe properly the glassy phase associated with the irreversibility phenomena observed experimentally.

## ACKNOWLEDGMENTS

The authors acknowledge partial financial support from Conselho Nacional de Desenvolvimento Científico e Tecnológico (CNPq) and Fundação de Amparo à Pesquisa do Estado de São Paulo (FAPESP).



- [1] D. Bertrand, A. R. Fert, M. C. Schmidt, F. Bensamka, and S. Legrand, *J. Phys. C* **15**, L883 (1982).
- [2] P. zen Wong, S. von Molnar, T. T. M. Palstra, J. A. Mydosh, H. Yoshizawa, S. M. Shapiro, and A. Ito, *Phys. Rev. Lett.* **55**, 2043 (1985).
- [3] P. zen Wong, H. Yoshizawa, and S. M. Shapiro, *J. Appl. Phys.* **57**, 3462 (1987).
- [4] H. Yoshizawa, S. Mitsuda, H. Aruga, and A. Ito, *Phys. Rev. Lett.* **59**, 2364 (1987).
- [5] H. Yoshizawa, S. Mitsuda, H. Aruga, and A. Ito, *J. Phys. Soc. Jpn.* **58**, 1416 (1989).
- [6] D. Sherrington and S. Kirkpatrick, *Phys. Rev. Lett.* **35**, 1792 (1975).
- [7] I. Y. Korenblit and E. F. Shender, *Zh. Éksp. Teor. Fiz.* **89**, 1785 (1985) [*Sov. Phys. JETP* **62**, 1030 (1985)].
- [8] Y. V. Fyodorov, I. Y. Korenblit, and E. F. Shender, *J. Phys. C* **20**, 1835 (1987).
- [9] Y. V. Fyodorov, I. Y. Korenblit, and E. F. Shender, *Europhys. Lett.* **4**, 827 (1987).
- [10] H. Takayama, *Prog. Theor. Phys.* **80**, 827 (1988).
- [11] J. M. Kincaid and E. G. D. Cohen, *Phys. Rep.*, *Phys. Lett.* **22C**, 57 (1975).
- [12] J. R. L. de Almeida and D. J. Thouless, *J. Phys. A* **11**, 983 (1978).
- [13] G. Parisi, *J. Phys. A* **13**, 1101 (1980).
- [14] G. Parisi, *J. Phys. A* **13**, 1887 (1980).
- [15] H. Yoshizawa, H. Mori, H. Kawano, H. Aruga-Katori, S. Mitsuda, and A. Ito, *J. Phys. Soc. Jpn.* **63**, 3145 (1994).
- [16] S. Fishman and A. Aharony, *J. Phys. C* **12**, L729 (1979).
- [17] J. L. Cardy, *Phys. Rev. B* **29**, 505 (1984).
- [18] P. zen Wong, S. von Molnar, and P. Dimon, *J. Appl. Phys.* **53**, 7954 (1982).
- [19] D. P. Belanger, in *Recent Progress in Random Magnets*, edited by D. H. Ryan (World Scientific, Singapore, 1992), pp. 277–308.
- [20] E. P. Raposo, M. D. Coutinho-Filho, and F. C. Montenegro, *Europhys. Lett.* **29**, 507 (1995).
- [21] E. P. Raposo and M. D. Coutinho-Filho, *Phys. Rev. B* **57**, 3495 (1998).
- [22] D. P. Belanger, W. E. Murray, Jr., F. C. Montenegro, A. R. King, V. Jaccarino, and R. W. Erwin, *Phys. Rev. B* **44**, 2161 (1991).
- [23] F. C. Montenegro, A. R. King, V. Jaccarino, S.-J. Han, and D. P. Belanger, *Phys. Rev. B* **44**, 2155 (1991).
- [24] K. Binder and A. P. Young, *Rev. Mod. Phys.* **58**, 801 (1986).
- [25] K. H. Fischer and J. A. Hertz, *Spin Glasses* (Cambridge University Press, Cambridge, 1991).
- [26] Y. Ma, C. Gong, and Z. Li, *Phys. Rev. B* **43**, 8665 (1991).
- [27] R. F. Soares, F. D. Nobre, and J. R. L. de Almeida, *Phys. Rev. B* **50**, 6151 (1994).
- [28] E. Nogueira, Jr., F. D. Nobre, F. A. da Costa, and S. Coutinho, *Phys. Rev. E* **57**, 5079 (1998); **60**, 2429(E) (1999).
- [29] J. Kushauer and W. Kleemann, *J. Magn. Magn. Mater.* **140-144**, 1551 (1995).
- [30] T. Schneider and E. Pytte, *Phys. Rev. B* **15**, 1519 (1977).
- [31] A. Aharony, *Phys. Rev. B* **18**, 3318 (1978).
- [32] J. R. L. de Almeida and R. Bruinsma, *Phys. Rev. B* **35**, 7267 (1987).
- [33] M. Mézard and A. P. Young, *Europhys. Lett.* **18**, 653 (1992).
- [34] M. Mézard and R. Monasson, *Phys. Rev. B* **50**, 7199 (1994).